Condensed Matter Physics.
General Relativity and Gravity

UDC 551.46; 53.09 https://www.doi.org/10.33910/2687-153X-2021-2-4-141-148

Statistical and spectral analysis of wind power: Fractional oscillation dynamics

A. F. Belo✉[1], K. Shimakawa[2]

[1] East Timor National University, Av. Cidade de Lisboa, Díli, East Timor
[2] Gifu University, 1–1 Yanagido, Gifu 501-1193, Japan

Authors
Abelito F. Belo, e-mail: abelitofilipe@gmail.com
Koichi Shimakawa, e-mail: koichi@gifu-u.ac.jp

For citation: Belo, A. F., Shimakawa, K. (2021) Statistical and spectral analysis of wind power: Fractional oscillation dynamics. *Physics of Complex Systems*, 2 (4), 141–148. https://www.doi.org/10.33910/2687-153X-2021-2-4-141-148
Received 3 September 2021; reviewed 22 September 2021; accepted 22 September 2021.
Funding: This work has been performed within JICA-CADEFEST 2 project.

Abstract. Time-dependent changes of the wind speed, as for example in Hera Campus (East Timor), are analysed by the statistical and the autocorrelation function in time domain and by the frequency spectrum (frequency domain) using the Fast Fourier Transform (FFT). The wind speed can be modelled using the Weibull distribution function. The autocorrelation function in time domain shows roughly a non-exponential decay with periodicity. The power spectrum shows two peaks and nearly $1/f^{\alpha}$ nature at high frequencies, close to the Kolmogorov prediction with $\alpha = 5/3$. A Cole-Davidson type generalisation of wind dynamics, originating from the fractional dynamics of oscillation, is different from the dynamics of tides.

Keywords: wind power, statistical analysis, Weibull probability distribution, autocorrelation function, Kolmogorov spectrum.

Introduction

Wind power should be one of the major inputs for producing sustainable environmental conditions of globe (Hasche 2010; Joselin Herbert et al. 2007). Worldwide wind power generation is now increasing significantly. Wind turbines are often used in large-scale wind farms in the countryside or in coastal regions. However, there has been a growing market for small-scale local farms with large numbers, evolving commercially helpful (Murthy, Rahi 2014; Norheim, Pudjianto 2008).

Wind power, however, is not stable, and the power produced by turbines varies with time. We should know the characteristic feature of variations in the local wind farms, because the nature of wind depends highly on locations. There are several ways to analyse wind characters in time and/or frequency domain. In the time domain, one simple way is to construct statistically a histogram of the step size (wind speed etc.) in output over time (Murthy, Rahi 2014; Wan, Bucaneg 2002). To understand the nature of *wind quality*, introducing the autocorrelation function (AF) can be useful. The other is to elucidate frequency spectrum (FS) (power spectrum) in frequency domain, which is helpful to understand the nature of wind power in details. From the AF and FS, it is easy to know randomness and periodicity of the wind power (Apt 2007).

In the present paper, as a series report of the tide dynamics (Belo et al. 2021), by using a small-size wind generator, we elucidate the nature of wind power at the Hera campus, Universidade Nacional Timor Lorosa'e, East Timor (8.55° S, 125.56° E). The wind speed variations throughout three months (June to September 2019) will be characterised in terms of a histogram, a probability distribution, and a power spectrum through the Fast Fourier Transform (FFT). The power spectrum shows two peaks (half and full days) with the high frequency tail of $1/f^{\alpha}$. The a-value closes to 5/3, which is known to be the Kolmogorov parameter found in turbulence (Apt 2007). It is discussed that the physical origin of the parameter a lies in the fractional dynamics of wind power, which leads to the Cole-Davidson type relaxation (Nigmatullin, Ryabov 1997). This is different from the dynamics of tide (Belo et al. 2021), in which a Lorentz-type relaxation is found in the frequency domain.

The autocorrelation function will be also elucidated from the time variation of wind speed, showing how much randomness is involved in the examined wind power (Belu, Koracin 2013). It is shown that the correlation time (memory effect of wind) is around 6 h, which may be related to the duration of Kolmogorov's turbulence.

Experimental and analytical technique

The data analysed in this work were collected between June 2019 and September 2019. Fig. 1 shows the 600-watt wind generator set (Nantong R&X Energy Technology: RX — 600H3) at Hera campus located 10 km east of Dili city.

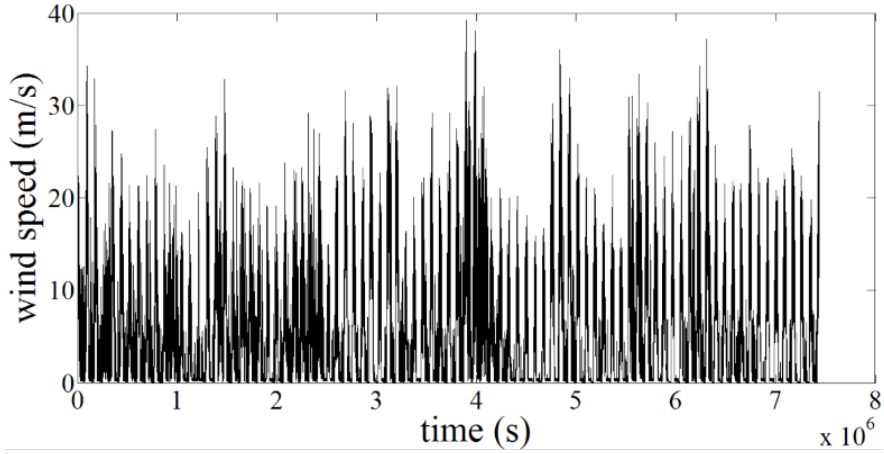

Fig. 1. Time-variation of the wind speed $v(t)$ at every 100 seconds for three months (8×10^6 s) at Hera campus (June to September 2019)

Wind speed was measured at the 6 m tall instrumented towers. The output voltage of wind turbine was transferred to the Data Logger (DL) (Belo et al. 2020). Data of the wind speed at every 100 seconds were stored in the PC. Collected data with the DL were Fourier transformed (Fast Fourier Transform: FFT). Fourier analysis converts a signal from its original time domain to the frequency domain. The FT of a time-dependent function $v(t)$ is given by

$$v(f) = \int_{-\infty}^{\infty} v(t) e^{-i2\pi ft} dt, \tag{1}$$

where $v(f)$ is the Fourier spectrum and f the frequency (s^{-1}) (Papoulis 1962). The FFT is an algorithm that computes the discrete $v(f)$ (Zonst 2004). Data of the wind speed at every 100 seconds for 3 months (data number N = 74398) are Fourier transformed using the MATLAB.

Elucidation of the autocorrelation function C(t) obtained, on the other hand, from the raw data is defined as

$$C(\tau) = \langle v(t) v(t+\tau) \rangle, \tag{2}$$

where < > is the time average, τ is called the correlation time. Note here that variation $v(t)$ is given as $v(t) = v'(t) - \langle v'(t) \rangle$, where $v'(t)$ is the raw data, giving therefore $\langle v(t) \rangle = 0$. When $\tau = 0$, $C(\tau) = C(0) = \langle v(t) v(t) \rangle = \langle v(t)^2 \rangle$, where $\langle v(t)^2 \rangle$ is called the *variance*.

 https://www.doi.org/10.33910/2687-153X-2021-2-4-141-148

$C(\tau) = 0$ means no correlation, i. e., no memory on a previous event after a time τ. The autocorrelation therefore shows to what extent the event in future is related to the past.

Results and discussion

Fig. 1 shows the measured time-dependent wind speed $v(t)$ at every 100 seconds for three months (8×10^6 s) at Hera campus (June to September 2019). The maximum wind speed is 35 m/s and the minimum is 0 m/s, with roughly 1-day periodicity (diurnal) and its second harmonics, which is a general trend in wind power reported in other areas (Apt 2007).

Fig. 2 shows the histogram for the wind speed $v(t)$ in which the probability density at a particular wind speed is obtained. The number of occurrences of each speed is counted for this object. Discrete bars shown in Fig. 2 present the wind speed distribution for the total number of data ($N_T = 74398$). It is known that the Weibull distribution is well-accepted and widely used for wind data analysis (Matsfelt, Davidson 2018; Murthy, Rahi 2014). We also find the wind speed follows the Weibull distribution given as

$$W(v) = A\frac{k}{c}\left(\frac{v}{c}\right)^{k-1} exp\left\{-\left(\frac{v}{c}\right)^{k}\right\}, \tag{3}$$

where k is called the shape parameter, c the scale parameter of the distribution, and k is the failure rate (Murthy, Rahi 2014). Note that A is just the fitting parameter to the number of frequency of histogram.

Dashed line in Fig. 2 shows the probability density $W(v)$ by taking the parameters $A = 10^5$, $c = 11.5$, and $k = 2.1$. Fitting with the histogram is reasonably good. A more accurate comparison between the data and the probability distribution function should be given by the integral form of the histogram producing just the probability (cumulative). Solid (black) and dash-dotted (red) lines in Fig. 2 show the probability calculated from the data (histogram) and the Weibull distribution (red dash line) using the same parameters. Both curves fit well, suggesting that the histogram (and hence the wind speed distribution) follows basically the Weibull distribution.

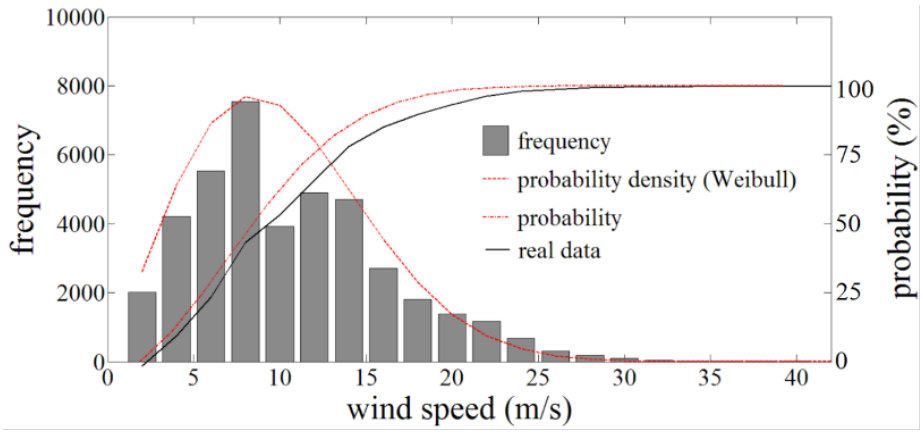

Fig. 2. Wind speed distribution (histogram) and the Weibull distribution

The power spectrum $|v(f)|^2$, obtained from the FFT, is shown in Fig. 3. At higher frequencies, it decreases with increasing frequency f and is approximately given by $1/f^{\alpha}$ by the thin solid line (red). The a-value and its functional origin will be discussed later. At lower frequencies, the spectrum shows a constant, which is often called a *low pass filter* (Belo et al. 2021). At around 10^{-5} Hz, a peak is observed, which corresponds to 1-day period. A 2nd harmonicity (peak) appears at half day cycle. It is not clear whether the presence of the 2nd harmonicity is due to a performance of the FFT or due to actual half-day cycle of the wind nature. We hence ignore the 2nd peak in the present analysis. Interestingly, the feature of $1/f^{\alpha}$ ($\alpha \sim 2$) at high frequencies has been found in the tidal-height spectrum at Dili port (Belo et al. 2021).

As stated already, the discussion of the autocorrelation function $C(\tau)$ may be helpful in understanding the underlying physics of the wind speed, which produces information on the periodicity and the memory of the time of events (Kogan 2008). Fig. 4 shows the autocorrelation functions for the imposed time shift,

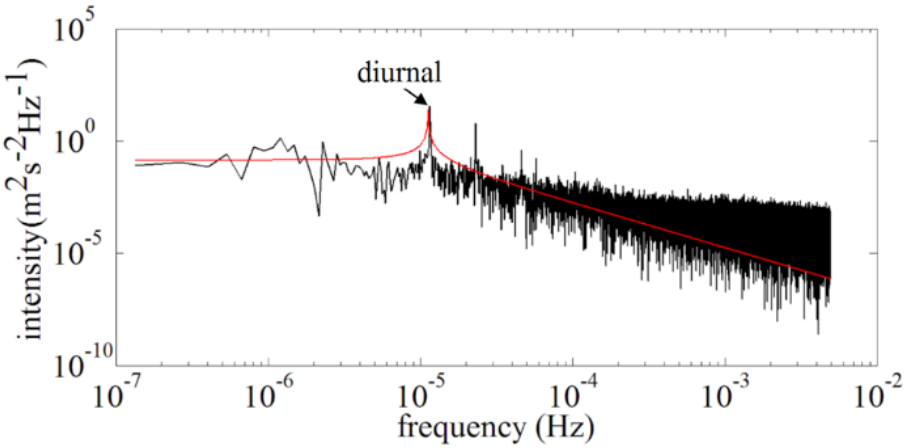

Fig. 3. Power spectrum $|v(f)|^2$ of $v(t)$ (shown in Fig. 1) obtained from the FFT. Solid line (red) is a model prediction of transfer function

(a) τ_{max} = 3.7 × 10^6 s (43 days) and for (b) τ_{max} = 1.8 × 10^5 s (~ two days). Here, we use the correlation time τ (not t) as a time variation. As seen for the $v(t)$ in Fig. 1, $C(\tau)$ shows the periodicity with beat. The time at which $C(\tau)$ is first crossing zero is a characteristic time τ_0 ($C(\tau)$ = 0), which is a measure of the time of losing memory of an event and is estimated to be 2.1 × 10^4 s (~ 6 h). We find the first (positive) peak at 8.7 × 10^4 s (~ 1 day) and the second one at 1.7 × 10^5 s (~ 2 days), indicating that there is a one-day periodicity (diurnal). A slow decrease in $C(\tau)$ with the time-lag around a half day indicates that the wind speed is not strictly periodic (Belu, Koracin 2013). A very slow decay of $C(\tau)$ suggests the presence of another periodic component of a much lower frequency.

Let us discuss the detailed nature of the power spectrum as shown in Fig. 3. As already stated, the power spectrum shows the principal peaks around at 10^{-5} Hz corresponding to the diurnal, and below and above these frequencies, it takes a constant value and is proportional to $1/f^{\alpha}$,respectively. The solid line (α = 2.0) is obtained from the following characteristic of an equivalent LRC electric circuit (EEC) as shown in Fig. 5 (a). The transfer function $H(\omega)$ (Draper et al. 2014), i. e. V_o/V_i for ω (= 2πf), is defined as

$$H(\omega)=\frac{V_o}{V_i}=\frac{\dfrac{R}{1+i\omega CR}}{\dfrac{R}{1+i\omega CR}+i\omega L}=\frac{1}{\left(1-\omega^2 CL\right)+i\omega\dfrac{L}{R}}\equiv\frac{1}{A+iB}\,, \tag{4}$$

where L is the inductance (H), R the resistance (Ω), and C the capacitance (F). A and B, respectively, are given as

$$A=1-\omega^2 CL=1-\frac{\omega^2}{\omega_0^2}\,, \tag{5}$$

$$B=\omega\frac{L}{R}=\omega\tau_c\,, \tag{6}$$

where ω_0 is the resonance frequency given by $1/(CL)^{1/2}$ and τ_c is the relaxation time given by L/R. The absolute value of $H(\omega)$ is then given by

$$\left|H(\omega)\right|=\left(\frac{1}{A^2+B^2}\right)^{\frac{1}{2}}. \tag{7}$$

The solid line shows the K·$|H(f)|$ with L = 2.0 × 10^4 (H), c = 1.0 × 10^4 (F), and R = 1.0 × 10^3 (Ω), where K is just an adjustable parameter (= 3.0 × 10^{-11}) to the data. The $|H(f)|$ takes a constant at low frequencies and is proportional to $1/f^{2.0}$ at high frequencies, with a peak at $2\pi f_0 = (LC)^{-1/2}$. Note, here, that second harmonics ($2f_0$) is not taken into account in the analysis. It is noted that fitting of $|H(f)|$ into the power

 https://www.doi.org/10.33910/2687-153X-2021-2-4-141-148

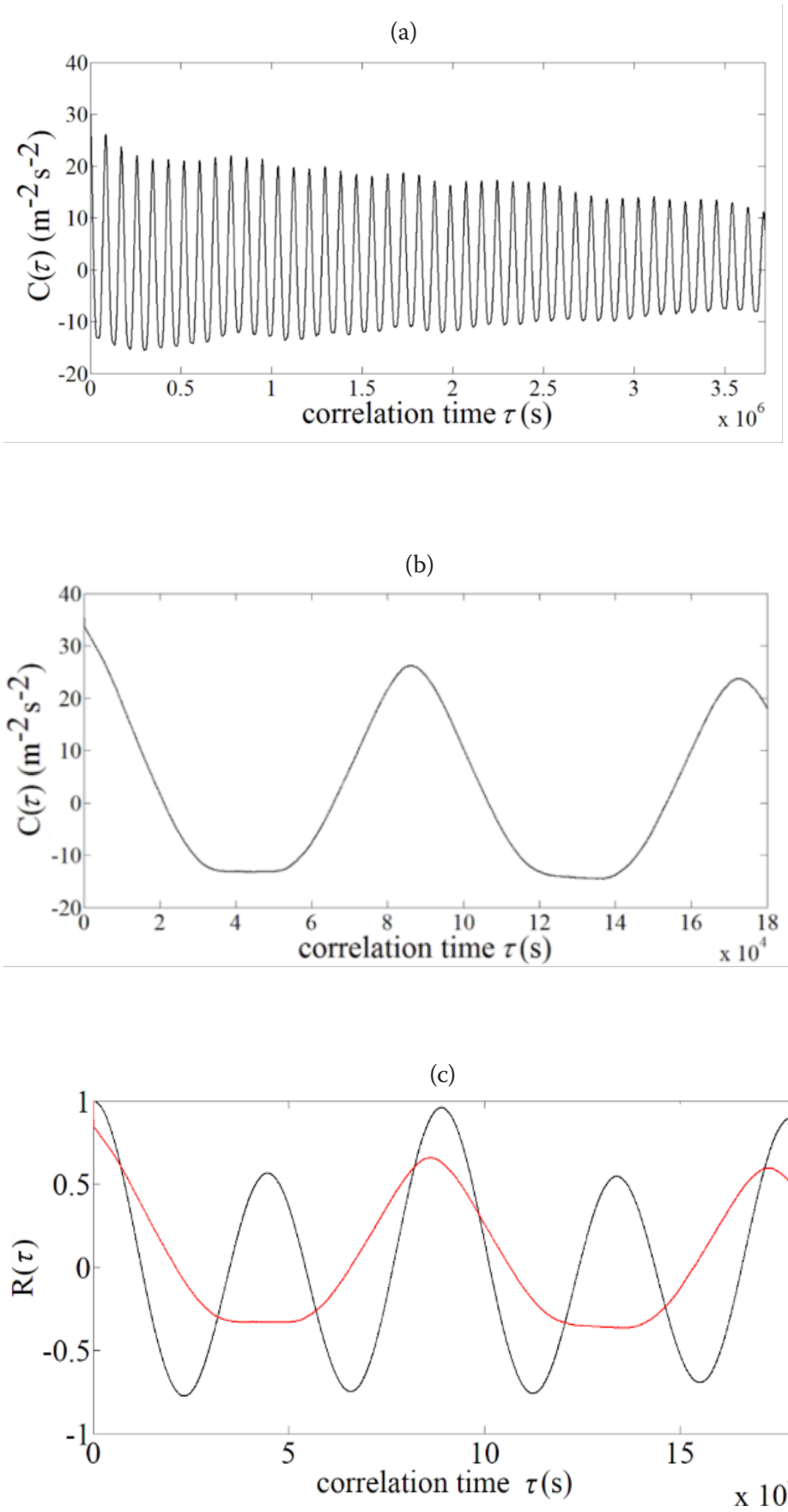

Fig. 4. Autocorrelation function of $v(t)$ for the imposed time shift, (a) $\tau_{max} = 3.7 \times 10^6$ s (43 days), for (b) $\tau_{max} = 1.8 \times 10^5$ s (~ two days) and for (c) tide (black) and wind power (red) for $\tau_{max} = 1.8 \times 10^5$ s (~ two days)

spectrum $|v(f)|^2$ at high frequencies is not good. Mind that the values for all physical parameters do not have any physical meaning, showing only the correspondence to an equivalent electrical circuit. A mechanical system is known to be equivalent to an electrical circuit: mass M (kg) corresponds to L, mechanical resistance R_m (kgs^{-1}) to R, and mechanical compliance C_m (mN^{-1} or $kg^{-1}s^2$) to C (Firestone 1933). Then the L, R, C in Eqs. (5), (6) and (7), can be replaced by these mechanical terms shown in Fig. 5 (b), when we discuss the wind dynamics.

The model predicts $1/f^{\alpha}$ ($\alpha = 2.0$) at higher frequencies with a peak (diurnal), while the actual spectrum shows $\alpha < 2.0$. It should be noted that *fractional kinetics* (*fractional calculus*) is discussed in some relaxation systems (Hilfer 2000; Nigmatullin, Ryabov 1997; Sokolov et al. 2002). The Cole-Davidson type relaxation (Nigmatullin, Ryabov 1997) found empirically in dielectric relaxation should be an example of fractional kinetics, while its origin is still not clear. The $H(\omega)$ can then be modified into

$$H(\omega) = \frac{1}{(A + iB)^{\beta}}, \tag{8}$$

where β ($0 < \beta < 1.0$) is the fractional parameter.

Solid line in Fig. 6 shows the power spectrum $|v(f)|2$ and $K \cdot |H(f)|$ (solid line) obtained from Eqs. (5), (6), and (8) with the parameters $f_0 = 1.13 \times 10^{-5}$ Hz, $\tau_0 = 20$ s, $\beta = 5/6$, and $K = 2.3 \times 10^{-13}$ (see Appendix). $K \cdot |H(f)|$ is proportional to $1/f^{2\beta}$. Note that $2\beta = 5/3$ is the well-known Kolmogorov's parameter on turbulence. We find that the Cole-Davidson type relaxation with $\beta = 5/6$ fits well into the practical power spectrum of the wind power at the present location. It should be mentioned that the wind power

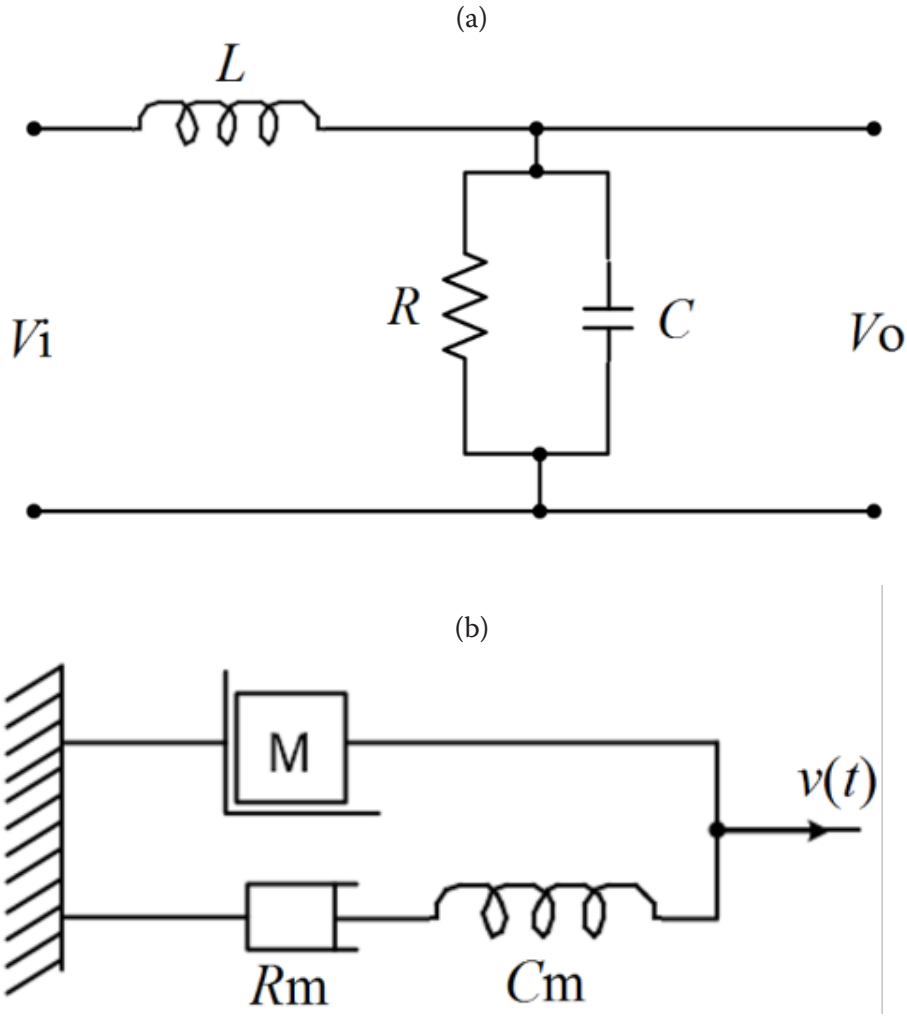

Fig. 5. (a) Equivalent electrical circuit on the wind dynamics, (b) Equivalent mechanical system

 https://www.doi.org/10.33910/2687-153X-2021-2-4-141-148

at the other locations also shows similar behaviour in which $1/f^{5/3}$ (Kolmogorov spectrum) has been reported (Apt 2007). Origin of the fractional dynamics of wind should be related to turbulence in wind nature (meteorological effect). Note in the tide dynamics that the power spectrum of tide in Dili port follows just 1/f at high frequencies, which is completely different from the present wind case. The tide dynamics is dominated only by the gravitational effect without involving the meteorological one (Belo et al. 2021).

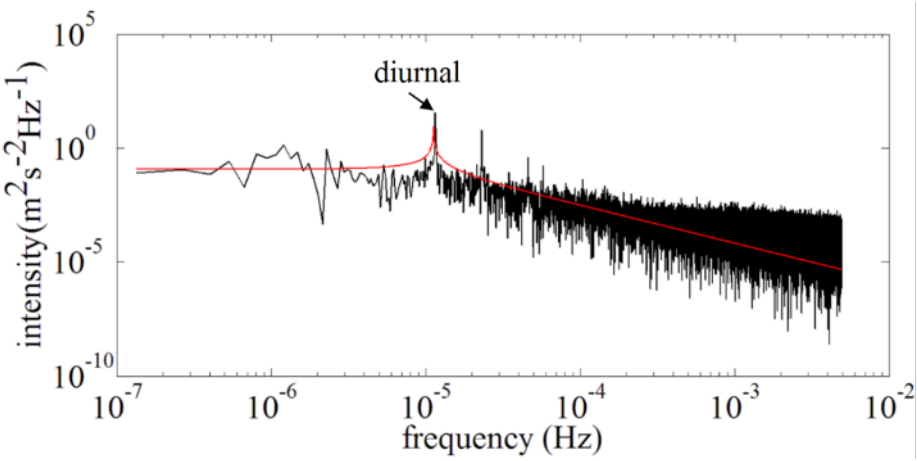

Fig. 6. Power spectrum of $v(t)$ from the FFT. Solid line (red) shows a model prediction (transfer function) of the fractional dynamics of wind power with α = 5/3

Conclusion

The variation of the wind speed during 3 months in time domain at Hera Campus (East Timor) was analysed through the histogram, AF, and FFT. The wind speed was modelled using the Weibull distribution function. The AF in time domain showed roughly a nonexponential decay with one-day periodicity and the correlation disappeared in 6 h. The power spectrum in frequency domain was approximately proportional to $1/f^{5/3}$ at higher frequencies (Kolmogorov spectrum), which was different from the tide dynamics. The Cole-Davidson type relaxation appearing in the wind spectrum should be highly related to turbulence and is related to the fractional dynamics.

Appendix

Equation (10) is solved in the following manner:

$$H(\omega) = (A + iB)^{-\beta} = (A^2 + B^2)^{-\frac{\beta}{2}} e^{-i(\beta \tan^{-1}\left(\frac{B}{A}\right)}$$
$$= (A^2 + B^2)^{-\frac{\beta}{2}} \left[\cos\left(\beta \tan^{-1}\frac{B}{A}\right) - i \sin\left(\beta \tan^{-1}\frac{B}{A}\right) \right],$$

where A and B are given Eqs. (5) and (6), respectively.

Conflict of Interest

The authors declare that there is no conflict of interest, either existing or potential.

Acknowledgement

We would like to thank Professors T. Kobayashi and Y. Takahashi for discussion on the weather focusing.

References

Apt, J. (2007) The spectrum of power from wind turbines. *Journal of Power Sources*, 169 (2), 369–374. https://doi.org/10.1016/j.jpowsour.2007.02.077 (In English)

Belo, A. F., Guterres, R., Pires, A., Shimakawa, K. (2020) Statistical and spectral analysis of wind power in hera campus. *Timorese Academic Journal of Science and Technology*, 3, 22–27. (In English)

Belo, A. F., Sasa, K., Marques, J. M., Shimakawa, K. (2021) Tide level in time and frequency domains at Dili port : Characteristic feature of a Lorentz oscillator. *Physics of Complex Systems*, 2 (1), 41–48. https://www.doi.org/10.33910/2687-153X-2021-2-1-41-48 (In English)

Belu, R., Koracin, D. (2013) Statistical and spectral analysis of wind characteristics relevant to wind energy assessment using tower measurements in complex terrain. *Journal of Wind Energy*, 2013, article 739162. http://dx.doi.org/10.1155/2013/739162 (In English)

Draper, S., Adcock, T. A., Borthwick, A. G., Houlsby, G. T. (2014) An electrical analogy for the Pentland Firth tidal stream power resource. *Proceedings of the Royal Society A*, 470 (2161), article 20130207. https://doi.org/10.1098/rspa.2013.0207 (In English)

Firestone, F. A. (1933) A new analogy between mechanical and electrical systems. *The Journal of the Acoustical Society of America*, 4, 249–267. https://doi.org/10.1121/1.1915605 (In English)

Hasche, B. (2010) General statistics of geographically dispersed wind power. *Wind Energy*, 13 (8), 773–784. https://doi:10.1002/we.397 (In English)

Hilfer, R. (2000) *Applications of fractional calculus in physics*. Singapore: World Cientific Publ., 472 p. https://doi.org/10.1142/3779 (In English)

Joselin Herbert, G. M., Iniyan, S., Sreevalsan, E., Rajapandian, S. (2007) A review of wind energy technologies. *Renewable and Sustainable Energy Reviews*, 11 (6), 1117–1145 https://doi.org/10.1016/j.rser.2005.08.004 (In English)

Kogan, Sh. (2008) *Electronic noise and fluctuations in solids*. Cambridge: Cambridge University Press, 367 p. (In English)

Matsfelt, J., Davidson, L. (2021) Large eddy simulation: A study of clearings in forest and their effect on wind turbines. *Wind Energy*. [Online]. https://doi.org/10.1002/we.2637 (accepted 28.08.2021). (In English)

Murthy, K. S. R., Rahi, O. P. (2014) Estimation of Weibull parameters using graphical method for wind energy applications. In*: 18th National power systems conference (NPSC–2014)*. Guwahati: IEEE Publ., pp. 1–6. https://www.doi.org/10.1109/NPSC.2014.7103858 (In English)

Nigmatullin, R. R., Ryabov, Ya. E. (1997) Cole-Davidson dielectric relaxation as a self-similar relaxation process. *Physics of Solid State*, 39 (1), 87–90. https://doi.org/10.1134/1.1129804 (In English)

Norheim, I., Pudjianto, D. (2007) Method for assessing impact of large-scale wind power integration on reserves. *Wind Energy*, 11 (1), 85–96. https://doi.org/10.1002/we.252 (In English)

Papoulis, A. (1962) *The fourier integral and its applications*. New York: McGraw-Hill Publ., 318 p. (In English)

Sokolov, I., Klafter, Y., Blumen, A. (2002) Fractional kinetics. *Physics Today*, 55 (11), 48–54. https://doi.org/10.1063/1.1535007 (In English)

Wan, Y., Bucaneg , D. Jr. (2002) Short-term power fluctuations of large wind power plants. *Journal of Solar Energy Engineering*, 124 (4), 427–431. https://doi.org/10.1115/1.1507762 (In English)

Zonst, A. E. (2004) *Understanding the FFT applications: A tutorial for students & working engineers*. 2nd ed., rev. Titusville: Citrus Press., 280 p. (In English)